AIP | The Journal of Chemical Physics

The lowest triplet state 3A′ of H3+: Global potential energy surface and vibrational calculations

Cristina Sanz, Octavio Roncero, César Tablero, Alfredo Aguado, and Miguel Paniagua

Citation: J. Chem. Phys. **114**, 2182 (2001); doi: 10.1063/1.1336566
View online: http://dx.doi.org/10.1063/1.1336566
View Table of Contents: http://jcp.aip.org/resource/1/JCPSA6/v114/i5
Published by the American Institute of Physics.

JOURNAL OF CHEMICAL PHYSICS VOLUME 114, NUMBER 5 1 FEBRUARY 2001

The lowest triplet state $^3A'$ of H_3^+: Global potential energy surface and vibrational calculations

Cristina Sanz and Octavio Roncero
Instituto de Matemáticas y Física Fundamental, C.S.I.C., Serrano 123, 28006 Madrid, Spain

César Tablero
Departamento de Ingeniería Electrónica, E.T.S.I. de Telecomunicación, Universidad Politécnica de Madrid, 28040 Madrid, Spain

Alfredo Aguado and Miguel Paniagua[a)]
Departamento de Química Física, Facultad de Ciencias C-XIV, Universidad Autónoma de Madrid, 28049 Madrid, Spain

(Received 9 August 2000; accepted 7 November 2000)

The adiabatic global potential energy surface of the H_3^+ system for the lowest triplet excited state of A' symmetry was computed for an extensive grid of conformations around the minimum region at full configuration interaction *ab initio* level, using a much more extended basis set than in a previous paper from the same authors. An accurate global fit (rms error lower than 27 cm^{-1} for energies lower than dissociation into separated atoms and lower than 5 cm^{-1} for energies lower than the dissociation channel) to these *ab initio* points and also to part of the previous calculated points (for a total of 7689 energies in the data set) of the lowest triplet excited state of A' symmetry is obtained using a diatomics-in-molecules approach corrected by one symmetrized three-body term with a total of 109 linear parameters and 1 nonlinear parameter. This produces an accurate global potential which represents all aspects of the bound triplet excited state of H_3^+ including the minima and dissociation limits, satisfying the correct symmetry properties of the system. The vibrational eigenstates have been calculated using hyperspherical coordinates with symmetry adapted basis functions with the proper regular behavior at the Eckart singularities. The accuracy of the vibrational levels thus obtained is expected to be better than 2 cm^{-1} with respect to unknown experimental values. Due to the presence of three equivalent minima at collinear geometries ($D_{\infty h}$) the lower vibrational levels are close to triple degenerate. Since the interconversion barrier between the three minima is about 2640 cm^{-1}, these states split for the upper excited vibrational levels. Such splitting can provide a key feature to identifying the unassigned transitions amongst the many H_3^+ lines that have been observed in hydrogen plasmas. [DOI: 10.1063/1.1336566]

I. INTRODUCTION

In a recent review on H_3^+, Tennyson[1] points out that it is possible that amongst the many H_3^+ lines that have been observed in hydrogen plasmas, some will belong to the lowest triplet excited state of H_3^+. But in the absence of a full potential energy surface for this state and sophisticated rovibrational calculations, these transitions will remain among the many that have yet to be assigned. McNab[2] also considers that no accurate calculations of vibration–rotation levels and no spectroscopic observations, which involve the triplet excited state of H_3^+, have been reported and such calculations and observations would be extremely interesting. Moreover, in a study of the infrared predissociation spectrum of the H_3^+ ion containing nearly 27 000 lines which span only 222 cm^{-1}, Carrington and Kennedy[3] note that H_3^+ has a bound excited triplet state in which the configuration is expected to be linear. Calculations suggest that this state is sufficiently stable to support a number of vibrational levels. However, they have not found evidence that the observed spectrum involves this triplet state. Therefore, any information on the rotation–vibration spectrum of the metastable triplet state of H_3^+ would be interesting.

Schaad and Hicks[4] were the first to locate an excited electronic state of H_3^+ that was bound with respect to vibration, the linear triplet state, which dissociates to $H_2^+(^2\Sigma_g^+) + H(^2S)$. Ahlrichs *et al.*[5] used a harmonic oscillator approximation to the potential energy surface near the minimum to determine the harmonic frequencies, force constants, as well as the formation energy of the reaction: $H_2^+(^2\Sigma_g^+) + H(^2S) \rightarrow H_3^+(^3\Sigma_u^+)$, which they estimate to be -8.43 kcal/mol. The most accurate calculation of the equilibrium properties of the triplet state of H_3^+ is by Preiskorn *et al.*,[6] who applied a hylleraas configuration interaction (HCI) method using an extended basis set $(14s5p1d)$ and obtained the best variational energy reported so far ($-1.116\,102\,7$ a.u.). Finally, their results are very close to Ahlrich *et al.*'s results.

A potential energy surface (PES) for the lowest triplet state of H_3^+ was reported by Wormer and de Groot.[7] They calculated about 400 points and gave a bidimensional analytic fit based on only 240 points using a modest uncontracted $(5s3p)$ Gaussian-type orbital basis set. The potential

[a)]Electronic mail: miguel.paniagua@uam.es

is expanded in terms of elements of Wigner's *D* matrices depending on hyperspherical angles maintaining a fixed hyper-radius (ρ). The authors conclude that the fitted PES does not have spectroscopic accuracy.[7] The authors also remark that a good description of the PES requires many configuration interaction calculations due to the presence of a narrow gorge in the PES that is otherwise very flat having a high probability of tunneling between the three symmetry-related minima. Moreover, they comment that the harmonic approximation used by previous researchers is inappropriate given the anharmonicity of the surface. However, no accurate calculations of rovibrational levels supported by this PES have been published.

In a previous paper,[8] hereafter referred as paper I, we reported full configuration interaction (FCI) *ab initio* calculations for a huge number of H_3^+ configurations and for a total of 36 states of A' and A'' irreducible representations with both singlet and triplet multiplicities. In paper I we also reported an accurate full dimensional analytical representation of the adiabatic ground-state $1\,^1A'$ global PES (GPES) and the corresponding rovibrational analysis. In the present paper our aim is to report a similar study for the lowest triplet excited state of the H_3^+ system.

II. POTENTIAL ENERGY CALCULATIONS

In paper I we reported FCI calculations using the extended $(11s6p2d)/[8s6p2d]$ basis set for a total of 8469 different H_3^+ conformations. We used the C_s symmetry group for all the geometries and had computed 36 different states at each point of A' and A'' irreducible representations with both singlet and triplet multiplicities. However, those calculations were made using a grid adapted to the adiabatic ground state $1\,^1A'$. In the case of the lowest triplet excited state $1\,^3A'$ both the repulsive wall and the shallow well are located at larger H–H distances than that corresponding to the ground state. As a consequence, those previous calculations corresponding to very short H–H distances must be discarded or weighted with a very small value for the fit. Moreover, the presence of a narrow gorge in the PES of the lowest triplet excited state $1\,^3A'$, reported by Wormer and de Groot,[7] requires many calculations to obtain a good description of such region. Therefore, we have computed a new set of FCI calculations for different H_3^+ conformations adapted to give a better description of the lowest triplet excited state mainly at the shallow well region.

The need for new calculations using more extended basis sets is also due to the need for a reliable estimate of the accuracy of the data corresponding to the lowest triplet excited state considered in this paper. The best reported variational result[6] corresponds to the minimum configuration and the basis set used in this case was of lower size than that used in the calculations reported in paper I. Moreover, the authors of the HCI calculations[6] claim that the importance of electron correlation for the triplet state is much lower than for the singlet state because the existence of the exchange hole is already accounted for in the conventional CI wave function. They also have noticed this effect in their study of the triplet excited states of H_2.[9] This effect means that the greater amount of improvement for the HCI energy in comparison to the FCI energy is due to the basis set size. We have calculated the FCI energy corresponding to the absolute minimum of the lowest triplet excited state, with the distance between two hydrogen atoms kept fixed at 2.454 bohr in a linear configuration, using as basis set the d-aug-cc-pV6Z[10] $(12s7p6d5f4g3h)/[8s7p6d5f4g3h]$ with a total of about 500 basis functions for this system. The resulting FCI energy with the above-mentioned basis set is $-1.116\,106\,27$ a.u. and, to our knowledge, is the best variational result reported so far—it is only about 1 cm^{-1} lower than the previous HCI result. Moreover, if we do the same calculation using the cc-pV6Z[10] basis set $(10s5p4d3f2g1h)/[6s5p4d3f2g1h]$, with less than 300 basis functions for this system, we obtain a total energy that is about 2 cm^{-1} higher than our best FCI result. Therefore, we select the latter cc-pV6Z basis to perform calculations at about 400 different configurations close to the minimum region to obtain an estimate of the accuracy of our data corresponding to the lowest triplet excited state.

To specify our grids of H_3^+ conformations, for our new FCI calculations on the lowest triplet excited state, we have adopted internal coordinates given by r_{12}, r_{13}, and the θ angle (θ being the $H_2\widehat{H_1}H_3$ corresponding angle in internal coordinates). The grid covering the shallow well was constructed by (all distances in bohr)

$$r_{12}=2.154+0.100i \quad (i=1,9),$$
$$r_{13}=2.154+0.100j \quad (j=i,9),$$

corresponding to 45 H_3^+ conformations for each θ angle that we have computed from collinear to perpendicular arrangements in increments of 10°. The total number of different conformations was 405. We use the $(11s6p2d)/[8s6p2d]$ basis set of paper I, along with cc-pV6Z[10] to compute the FCI data points. We have used C_s symmetry group for all the geometries. Using the $(11s6p2d)$ basis set, with the four innermost *s* functions contracted to $[8s6p2d]$, the total energy of H_3^+ at its lowest triplet excited-state equilibrium geometry (linear symmetric conformation, equilibrium bond length R_e=2.454 bohr) is $-1.116\,046$ a.u., about 13 cm^{-1} above the best variational result reported in this paper. However, as we stressed in paper I, this absolute error is not as important as the error in energy differences with respect to a reference zero energy. Since we have computed the same conformations using the cc-pV6Z basis set, it is possible to obtain a rms deviation of our energy difference errors, taken as zero energy value the corresponding energy of the equilibrium geometry both for the $(11s6p2d)/[8s6p2d]$ energy differences (zero energy at $-1.116\,046$) as for the cc-pV6Z more accurate energy differences (zero energy at $-1.116\,098$). The resulting rms deviation is less than 5 cm^{-1} (and only about 15 cm^{-1} if the rms is calculated with respect to the absolute energies).

Including the FCI energies for the lowest triplet excited state, obtained in paper I, up to 70 000 cm^{-1} above the lowest triplet excited-state absolute minimum (zero energy at $-1.116\,046$ a.u.), we obtain a total number of 7689 conformations. Two files containing the 7689 lowest triplet excited-state H_3^+ data points used to obtain the GPES reported in this paper and the 405 very accurate cc-pV6Z energies mentioned earlier, have been placed in the electronic depository EPAPS.[11] We must stress that the dissociation channel corresponding to H_2^+ $(X\,^2\Sigma_g^+)$ + H (^2S) is about 2956 cm^{-1} above the first triplet excited-state minimum (4101 cm^{-1} when zero point energy of H_2^+, $X\,^2\Sigma_g^+$ is included) and the dissociation into the three separated atoms $(H,^2S+H,^2S+H^+)$ is 25 469 cm^{-1} above the H_3^+ $^3A'$ minimum, while we are considering all data up to 70 000 cm^{-1} above this minimum.

III. THE FIRST TRIPLET EXCITED-STATE H_3^+ GLOBAL SURFACE

We write the global potential energy surface corresponding to the H_3^+ first triplet excited state $(1\,^3A')$ as

$$V_{H_3^+}=V_{DIM}+\sum_{L}^{L_{max}} V_{ABC}^{(3)L}(R_{AB},R_{AC},R_{BC}), \qquad (1)$$

where V_{DIM} is the lowest eigenvalue of the symmetric 3×3 matrix, corresponding to the diatomics-in-molecules approach with neglected overlap, given by

$$H_{11}=V_{AB}^{(2)}(H_2,{}^3\Sigma_u^+)-2V_H^{(1)}+\tfrac{1}{2}[V_{AC}^{(2)}(H_2^+,{}^2\Sigma_g^+)+V_{AC}^{(2)}(H_2^+,{}^2\Sigma_u^+)+V_{BC}^{(2)}(H_2^+,{}^2\Sigma_g^+)+V_{BC}^{(2)}(H_2^+,{}^2\Sigma_u^+)],$$

$$H_{22}=V_{AC}^{(2)}(H_2,{}^3\Sigma_u^+)-2V_H^{(1)}+\tfrac{1}{2}[V_{AB}^{(2)}(H_2^+,{}^2\Sigma_g^+)+V_{AB}^{(2)}(H_2^+,{}^2\Sigma_u^+)+V_{BC}^{(2)}(H_2^+,{}^2\Sigma_g^+)+V_{BC}^{(2)}(H_2^+,{}^2\Sigma_u^+)],$$

$$H_{33}=V_{BC}^{(2)}(H_2,{}^3\Sigma_u^+)-2V_H^{(1)}+\tfrac{1}{2}[V_{AB}^{(2)}(H_2^+,{}^2\Sigma_g^+)+V_{AB}^{(2)}(H_2^+,{}^2\Sigma_u^+)+V_{AC}^{(2)}(H_2^+,{}^2\Sigma_g^+)+V_{AC}^{(2)}(H_2^+,{}^2\Sigma_u^+)],$$

$$H_{12}=\tfrac{1}{2}[V_{BC}^{(2)}(H_2^+,{}^2\Sigma_u^+)-V_{BC}^{(2)}(H_2^+,{}^2\Sigma_g^+)],$$

$$H_{13}=\tfrac{1}{2}[V_{AC}^{(2)}(H_2^+,{}^2\Sigma_u^+)-V_{AC}^{(2)}(H_2^+,{}^2\Sigma_g^+)],$$

$$H_{23}=\tfrac{1}{2}[V_{AB}^{(2)}(H_2^+,{}^2\Sigma_u^+)-V_{AB}^{(2)}(H_2^+,{}^2\Sigma_g^+)],$$

$V_H^{(1)}$ being the energy of the ^2S state of the H(1s) atom (−0.5 a.u. or −109 737 cm^{-1}).

The two-body energies $V_{AB}^{(2)}$ (including the nuclear repulsion) have been written as in paper I [see Eqs. (2)–(5) in paper I—note that in paper I there is a misprint in the off-diagonal terms of the DIM matrix, which must be changed of sign; this misprint did not affect the results of the paper]. The linear and nonlinear parameters are determined also as explained in paper I. In Table I we report the parameters corresponding to the H_2: $b\,^3\Sigma_u^+$ needed to construct the DIM surface along with the H_2^+: $X\,^2\Sigma_g^+$ and $1\,^2\Sigma_u^+$, which are exactly the same as used in paper I to construct the DIM surface corresponding to the ground state. The parameters corresponding to these two latter diatomic potentials have been reported in Tables II and III in paper I. We must stress that the V_{DIM} potential does not hold the shallow minima (there are three equivalent minima due to permutational symmetry) for the lowest triplet excited state at $D_{\infty h}$ geometries (linear symmetric) but it has minima at $C_{\infty v}$ (linear asymmetric). However, the V_{DIM} potential has the advantage, with respect to a simple sum of diatomic potentials, that it gives a good description of a conical intersection produced at D_{3h} geometries (equilateral triangles) between the two lower triplet excited states of H_3^+.

For the three-body terms of the global potential, $V_{ABC}^{(3)L}$ in Eq. (1), we choose the same expansion as that given in paper I [see Eqs. (6) and (7) in paper I], including the same symmetry constraints in the linear and nonlinear parameters, to ensure that the global potential is invariant with respect to permutations of all the equivalent nuclei.[12] We must emphasize that the symmetry treatment is analytical both for the three-body terms and the global potential. Therefore, the global potential is invariant with respect to permutations of all the equivalent nuclei.

In Table II we present the rms values for different fits of the global H_3^+ first triplet excited-state potential using only one three-body term [$L_{max}=1$, see Eq. (1)]. In this case the

TABLE I. Two-body[a] term $V^{(2)}(H_2,{}^3\Sigma_u^+)$.

i	c_i
0	0.115 702 741(+01)
1	0.539 794 080(+00)
2	0.414 449 834(+02)
3	−0.217 491 036(+04)
4	0.681 679 240(+05)
5	−0.131 911 745(+07)
6	0.163 372 038(+08)
7	−0.131 757 468(+09)
8	0.687 898 123(+09)
9	−0.223 982 910(+10)
10	0.413 123 247(+10)
11	−0.329 426 623(+10)
α_{HH}	0.197 399 300(+01)
$\beta_{HH}^{(2)}$	0.153 849 500(+01)

[a]All the coefficients are given in atomic units.

TABLE II. Accuracy vs the order (K) of the fit for several energy groups.

		Maximum energy[a]/(data points)		
K	n_{par}[b]	2956/(1292)	25 469/(5565) rms error (cm^{-1})	70 000/(7689)
3	3	407.79	1354.24	2411.66
4	6	112.68	605.08	1821.28
5	10	110.89	458.39	724.27
6	16	40.32	190.51	521.80
7	23	35.81	165.38	242.81
8	32	18.95	81.70	188.58
9	43	14.38	68.26	145.88
10	56	10.00	43.21	130.69
11	71	6.30	36.91	92.85
12	89	6.10	32.71	78.90
<u>13</u>	<u>109</u>	<u>4.65</u>	<u>26.65</u>	<u>63.42</u>
14	132	4.40	24.66	57.02
15	158	3.98	21.31	52.99

[a]Energies in cm^{-1}.
[b]n_{par} is the number of linear parameters of the fit.

gain in the accuracy of the fit when using more three-body terms is practically negligible. We fit the three-body term to $V_{H_3^+} - V_{DIM}$, where $V_{H_3^+}$ are given by the total 7689 data points. In Table II we can see that the accuracy of the fit reaches approximately the accuracy of the data points (that we have estimated about 5 cm^{-1}) for an expansion of order 13 with 109 linear parameters and 1 nonlinear parameter, if we consider the first group of 1292 data points with energy lower than the dissociation channel (2956 cm^{-1}). The rms increases to about 27 cm^{-1} when considering the group of 5565 data points with energy lower than the dissociation into separated atoms (25 469 cm^{-1}). Finally the rms corresponding to all data points (up to 70 000 cm^{-1}) is about 63 cm^{-1} (see the last column in Table II). Therefore, we select as a final fit the underlined in Table II (fit order $K=13$ with 109 linear parameters, 1 nonlinear parameter). In Table III we collect the parameters corresponding to this ''final'' fit. However, as we can see from Table II our fitting procedure is able to attain lower rms errors for the global fit (see the row corresponding to $K=15$).

In Fig. 1 potential energy contours of the H_3^+ lowest triplet excited-state GPES have been plotted using Jacobi coordinates in which **r** is the H_2 internuclear vector, **R** is the vector joining the center of mass of H_2 to the remaining H atom, and Θ is the angle between them. The GPES corresponding to the present results have been plotted for three different **r** values fixed at 2.454 bohr (top panel), 3.681 bohr (intermediate panel), and 4.908 bohr (bottom panel). In this Fig. 1 we have plotted (x,y) points where (0,0) corresponds to the center of mass of H_2 with the position of the two fixed nuclei indicated by a closed circle in the X axis. The corresponding **R** and Θ values correspond to: $\mathbf{R}=x^2+y^2$ and $\tan\Theta=y/x$. As we can see from Fig. 1 (top panel) two minima are present when the remaining H atom approaches the H_2 encounter at a linear configuration with the same distance (2.454 bohr) between them. In the bottom panel of Fig. 1 the third minimum is present for the insertion of the remaining H atom to the H_2 encounter at a linear configuration. The minimum location in this last case is at the (0,0) point. In the three panels of Fig. 1 we have indicated the contour corresponding to the energy of the interconversion barrier (i.e., the energy required to cross the barrier between linear structures with the atom ordering permuted, about 2640 cm^{-1}) using a thicker line.

Furthermore, in Fig. 2 we have plotted the same GPES as in Fig. 1, but now using a stereographic projection in hyperspherical coordinates.[13] The three hyperspherical coordinates are ρ, θ, and ϕ_τ.[13] The coordinate ρ can be said to describe the overall size of the system, and θ and ϕ_τ describe its shape. Pack and Parker[13] have noted that it is often advantageous to view the surface of the internal sphere as functions of θ and ϕ_τ with ρ fixed. The stereographic projection has X and Y defined as in paper I. The three internal coordinates, ρ, θ, and ϕ_τ, are easily related to Jacobi coordinates r_τ, R_τ, and Θ_τ, with $\tau=A,B,C$ (A,B,C denoting the three particles of interest), through the expressions given by the Eq. (8) in paper I. In all panels of Fig. 2, six arrangement channels appear instead of the expected three because of the inversion symmetry in the ϕ_τ coordinate, causing each channel to be repeated twice. In this Fig. 2 we have selected three fixed ρ values. The first one corresponds to the ground-state absolute minimum position ($\rho=2.20$ bohr, upper panel), which in this case corresponds to very high energies since the minimum location for the first triplet excited-state

TABLE III. Parameters of the three-body[a] terms $V^{(3)L}(L=1)$.

ijk	d_{ijk}	ijk	d_{ijk}
1 1 0	0.125 908 364 357(+00)	9 1 0	0.140 124 095 212(+09)
1 1 1	0.756 670 530 347(+03)	4 4 3	0.126 382 813 227(+10)
2 1 0	−0.100 785 011 345(+03)	5 3 3	0.125 742 377 361(+10)
2 1 1	−0.112 076 560 847(+05)	5 4 2	0.188 986 250 401(+10)
2 2 0	0.708 827 009 352(+03)	5 5 1	0.290 551 791 794(+10)
3 1 0	0.363 843 657 753(+04)	6 3 2	0.249 280 933 649(+09)
2 2 1	0.196 236 013 676(+06)	6 4 1	−0.150 957 274 478(+10)
3 1 1	0.667 223 607 363(+05)	6 5 0	−0.331 959 222 399(+09)
3 2 0	−0.239 095 814 122(+05)	7 2 2	0.392 467 127 301(+09)
4 1 0	−0.619 181 358 190(+05)	7 3 1	−0.298 164 436 741(+09)
2 2 2	−0.274 171 779 781(+07)	7 4 0	0.270 808 070 118(+09)
3 2 1	−0.138 020 020 716(+07)	8 2 1	0.772 059 381 489(+09)
3 3 0	0.105 231 724 008(+06)	8 3 0	−0.494 411 667 806(+09)
4 1 1	−0.201 094 263 862(+06)	9 1 1	−0.120 948 885 460(+10)
4 2 0	0.456 694 587 835(+06)	9 2 0	−0.107 795 498 319(+09)
5 1 0	0.646 677 771 549(+06)	10 1 0	−0.181 513 272 850(+09)
3 2 2	0.174 109 197 838(+08)	4 4 4	−0.115 286 341 864(+11)
3 3 1	0.121 406 743 571(+08)	5 4 3	0.245 176 499 103(+10)
4 2 1	0.384 414 789 312(+07)	5 5 2	0.439 753 355 704(+10)
4 3 0	−0.148 237 361 115(+07)	6 3 3	−0.421 255 975 763(+10)
5 1 1	0.793 913 653 520(+06)	6 4 2	−0.907 564 952 613(+10)
5 2 0	−0.423 277 302 358(+07)	6 5 1	−0.259 958 734 939(+10)
6 1 0	−0.451 511 960 519(+07)	6 6 0	0.143 113 520 510(+10)
3 3 2	−0.994 595 545 126(+08)	7 3 2	0.533 692 048 853(+10)
4 2 2	−0.586 606 796 348(+08)	7 4 1	0.545 015 147 815(+10)
4 3 1	−0.437 734 300 382(+08)	7 5 0	−0.607 842 427 815(+09)
4 4 0	0.637 840 592 224(+07)	8 2 2	−0.428 906 780 011(+10)
5 2 1	−0.396 324 915 426(+07)	8 3 1	−0.236 571 971 394(+10)
5 3 0	0.125 500 142 963(+08)	8 4 0	−0.279 183 725 298(+09)
6 1 1	−0.535 653 476 932(+06)	9 2 1	0.229 547 597 510(+09)
6 2 0	0.232 406 725 459(+08)	9 3 0	0.713 794 118 205(+09)
7 1 0	0.214 011 272 949(+08)	10 1 1	0.159 430 834 987(+10)
3 3 3	0.353 438 871 488(+09)	10 2 0	−0.153 066 620 515(+09)
4 3 2	0.333 305 056 649(+09)	11 1 0	0.140 732 353 373(+09)
4 4 1	0.281 240 527 905(+09)	5 4 4	0.299 844 281 174(+09)
5 2 2	0.814 253 944 928(+08)	5 5 3	0.221 356 762 873(+11)
5 3 1	−0.221 807 371 189(+08)	6 4 3	−0.167 852 560 565(+11)
5 4 0	−0.315 051 506 285(+08)	6 5 2	−0.469 020 697 255(+10)
6 2 1	0.540 032 411 141(+08)	6 6 1	0.831 078 811 250(+10)
6 3 0	−0.563 776 044 648(+08)	7 3 3	0.177 589 432 851(+11)
7 1 1	−0.530 935 436 616(+08)	7 4 2	0.127 131 680 936(+11)
7 2 0	−0.801 621 935 198(+08)	7 5 1	−0.442 987 038 373(+10)
8 1 0	−0.678 806 616 897(+08)	7 6 0	−0.799 971 961 308(+09)
4 3 3	−0.863 505 893 454(+09)	8 3 2	−0.121 197 982 775(+11)
4 4 2	−0.854 080 368 230(+09)	8 4 1	−0.252 251 250 157(+10)
5 3 2	−0.698 050 434 007(+09)	8 5 0	0.124 079 402 836(+10)
5 4 1	−0.507 210 133 526(+09)	9 2 2	0.797 183 898 765(+10)
5 5 0	0.191 908 924 241(+09)	9 3 1	0.327 566 454 838(+10)
6 2 2	0.452 586 159 086(+08)	9 4 0	−0.314 162 403 706(+09)
6 3 1	0.462 286 067 291(+09)	10 2 1	−0.153 363 336 919(+10)
6 4 0	0.397 247 773 540(+07)	10 3 0	−0.333 568 196 238(+09)
7 2 1	−0.383 896 684 511(+09)	11 1 1	−0.690 662 746 223(+09)
7 3 0	0.189 314 096 225(+09)	11 2 0	0.230 867 389 814(+09)
8 1 1	0.400 921 663 460(+09)	12 1 0	−0.562 803 837 614(+08)
8 2 0	0.158 449 830 423(+09)		
$\beta^{(3)L}$	0.108 230 230 000(+01)		

[a]All the coefficients are given in atomic units.

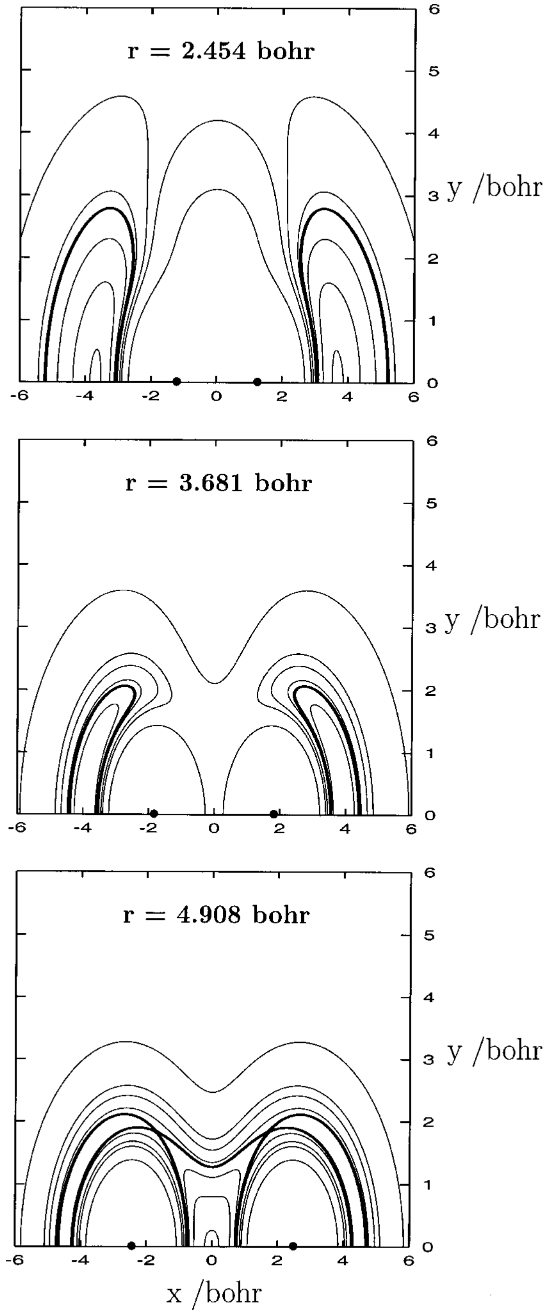

FIG. 1. Contours of the first triplet excited-state H_3^+ GPES in Jacobi coordinates **r**, **R**, and Θ. The *x* and *y* have been defined as: $x=\mathbf{R}\cos\Theta$, $y=\mathbf{R}\sin\Theta$. For each contour map the **r** distance is fixed (2.454 bohr for the upper panel, 3.681 bohr for the intermediate panel, and 4.908 bohr for the bottom panel). The solid curves are contours of the interaction potential corresponding to 100, 1000, 2000, 2640 (thicker line), 3000, 4000, 5000, and 10 000 cm^{-1}. Distances are given in bohr.

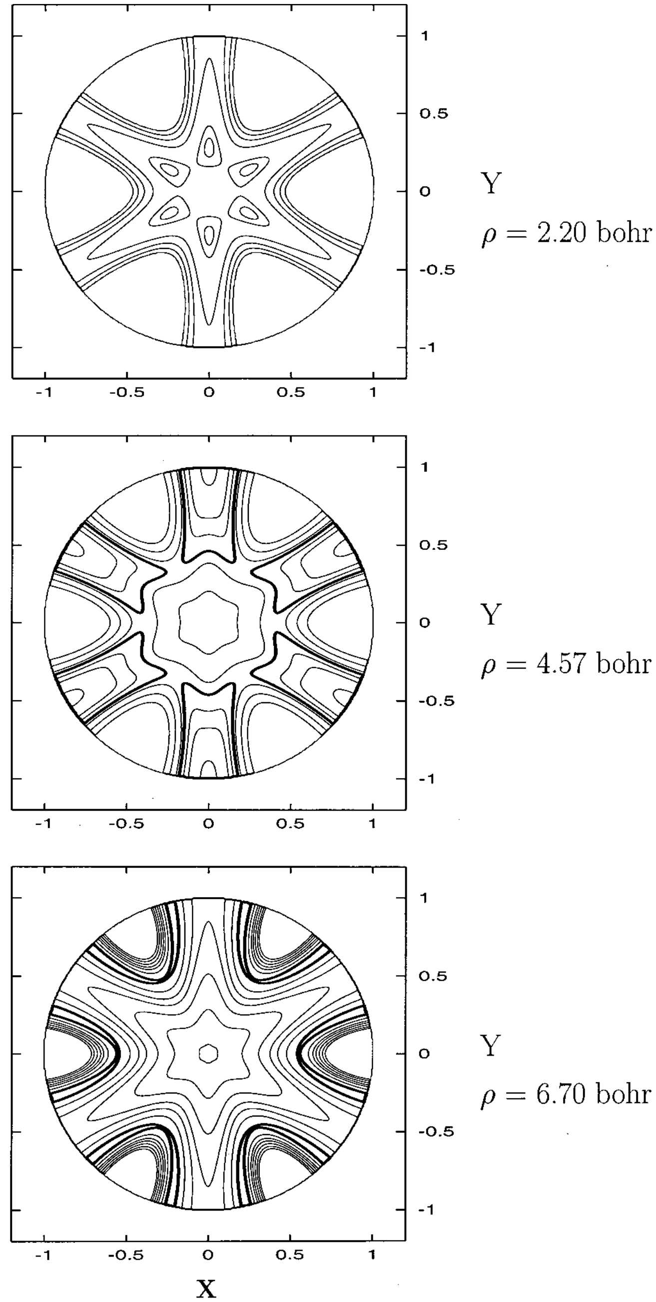

FIG. 2. Stereographic projection of contour plots of the first triplet excited-state H_3^+ GPES in hyperspherical coordinates ρ, θ, and ϕ_τ. The *x* and *y* have been defined as: $x=\tan(\theta/2)\cos(\phi_\tau)$ and $y=\tan(\theta/2)\sin(\phi_\tau)$. For each contour map the ρ distance is fixed (2.20 bohr for the upper panel, 4.57 bohr for the intermediate panel, and 6.70 bohr for the bottom panel). The solid curves are contours of the interaction potential. The contours are 58 500, 60 000, 70 000, 80 000, 90 000, and 100 000 cm^{-1} for the top panel, 100, 1000, 2000, 2640 (thicker line), 5000, 10 000, and 20 000 cm^{-1} for the intermediate panel, and 2640 (thicker line), 4000, 6000, 8000, 11 000, 15 000, and 19 500 cm^{-1} for the bottom panel.

is displaced to longer distances. The second one corresponds to the first triplet excited state absolute minimum position (ρ=4.57 bohr, intermediate panel). Here we have six minima (three minima repeated twice due to inversion symmetry in the ϕ_τ coordinate) located at the equatorial region, the contour connecting them corresponds to the interconversion barrier and is indicated in Fig. 2 by means of a thicker line. The third one (bottom panel) corresponds to a longer value of ρ corresponding to the interconversion barrier location (ρ=6.70 bohr). Here we can see that the lower energy contour (the thicker one in Fig. 2) connects the six channels. In all panels we can see that symmetry always has a good behavior due to the analytical treatment.

Finally, the main features of this GPES along with the corresponding GPES of the ground state (see paper I) are shown in Fig. 3, where we represent a qualitative energy diagram of the minimum energy path corresponding to the

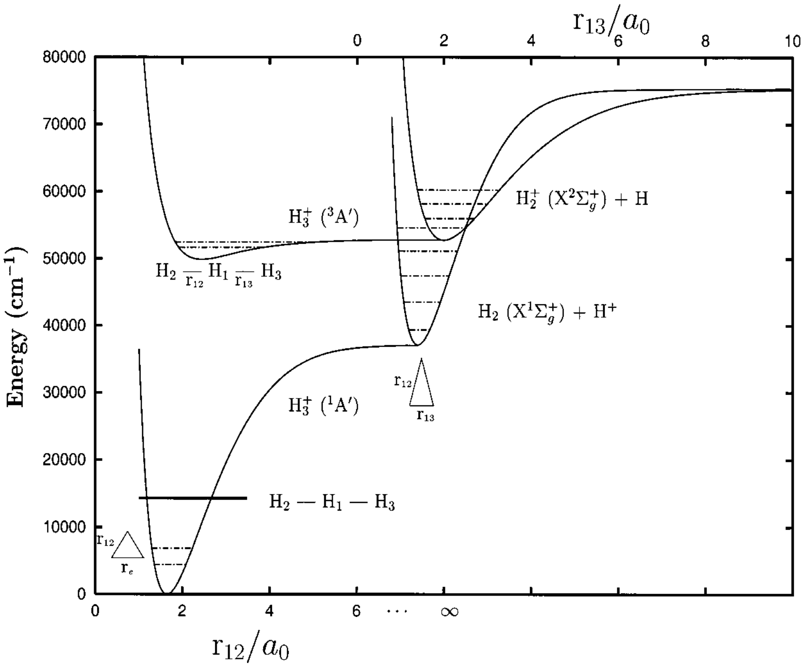

FIG. 3. Energy diagram of the minimum energy path for both ground and first triplet excited states of H_3^+. Zero energy is fixed at the absolute minimum of the ground state ($^1A'$). The minimum of the first excited triplet state ($^3A'$) is 49 833 cm^{-1} above the ground-state minimum and it is considered the zero energy, throughout the text, for the GPES reported in this paper.

ground state ($1\,^1A'$) and to the lowest triplet excited state ($1\,^3A'$). In this Fig. 3 we can see that the minimum corresponding to the first triplet excited state is 49 833 cm^{-1} above the absolute minimum of the ground state.

IV. VIBRATIONAL ANALYSIS OF THE H_3^+ LOWEST TRIPLET EXCITED STATE

The rovibrational states of H_3^+ are studied using the adiabatically adjusting principal axes hyperspherical coordinates of Pack and Parker,[14] (denoted by APHJ), which are closely related to those described by Smith[15,16] and Johnson.[17,18] In these coordinates the body-fixed frame coincides with the principal axis system and the z axis is perpendicular to the plane containing the three atoms. The orientation of the body-fixed frame relative to a space-fixed one is specified by three Eulerian angles, α, β, γ. The three internal coordinates, ρ, θ, ϕ_τ, are easily related to any of the three equivalent sets of Jacobi coordinates.[13] Therefore, the use of these coordinates is particularly well suited for treating the permutational symmetry of triatomic systems with three identical nuclei, which may yield a significant reduction of the size of the Hamiltonian matrices for a particular irreducible representation. Moreover, if the system presents three equivalent minima with a relatively low barrier, as is the case studied here, these coordinates give a simple description of the tunneling among them. Other coordinates, as Jacobi coordinates, have the disadvantage that the Hamiltonian present radial singularities for some linear geometries.[19]

In paper I, we used symmetry adapted functions using these coordinates to calculate rovibrational states of $H_3^+(^1A')$, up to high total angular momentum ($J=20$). In that case, the electronic state is totally symmetric and does not deserve special attention when dealing with the permutation symmetry. Here we present generalized symmetry adapted functions for treating electronic states with arbitrary symmetry. For doing that, in Table IV the effect of the dif-

TABLE IV. Effect of the symmetry operators on the nuclear (APHJ coordinates) and electronic coordinates and functions.

Symmetry operator	Euler angles	Internal APHJ coordinates	Electronic coordinates	Transformed functions
E	α,β,γ	ρ,θ,ϕ_τ	x_i,y_i,z_i	$W_{\Omega n}^{JM\Gamma S\sigma C_2}$
$\mathcal{P}_{AB}$	$\alpha+\pi,\pi-\beta,\pi-\gamma$	$\rho,\theta,2\pi/3-\phi_\tau$	$-x_i,y_i,-z_i$	$C_2(-1)^{J-\Omega}e^{i2n\pi/3}W_{-\Omega-n}^{JM\Gamma S\sigma C_2}$
$\mathcal{P}_{BC}$	$\alpha+\pi,\pi-\beta,\pi-\gamma$	$\rho,\theta,-\phi_\tau$	$-x_i,y_i,-z_i$	$C_2(-1)^{J-\Omega}W_{-\Omega-n}^{JM\Gamma S\sigma C_2}$
$\mathcal{P}_{CA}$	$\alpha+\pi,\pi-\beta,\pi-\gamma$	$\rho,\theta,-2\pi/3-\phi_\tau$	$-x_i,y_i,-z_i$	$C_2(-1)^{J-\Omega}e^{-i2n\pi/3}W_{-\Omega-n}^{JM\Gamma S\sigma C_2}$
$\mathcal{P}_{ABC}$	α,β,γ	$\rho,\theta,4\pi/3+\phi_\tau$	x_i,y_i,z_i	$e^{i4n\pi/3}W_{\Omega n}^{JM\Gamma S\sigma C_2}$
$\mathcal{P}_{ABC}^{-1}$	α,β,γ	$\rho,\theta,-4\pi/3+\phi_\tau$	x_i,y_i,z_i	$e^{-i4n\pi/3}W_{\Omega n}^{JM\Gamma S\sigma C_2}$
E^*	$\alpha,\beta,\gamma+\pi$	ρ,θ,ϕ_τ	$x_i,y_i,-z_i$	$\sigma(-1)^{\Omega}W_{-\Omega-n}^{JM\Gamma S\sigma C_2}$

TABLE V. Vibronic eigenvalues (in cm^{-1}) of H_3^+ for $J=0$ for the present GPES.

$i(\Gamma,J)$	A_2'	$i(\Gamma,J)$	A_1'	$i(\Gamma,J)$	E'	(v_1,v_2,v_3) $(\sigma_u^+,\sigma_g^+,\pi_u)$
1	1719.2728		⋯	1–2	1719.2728	0 0 0
	⋯	1	2455.620	3–4	2455.618	0 0 1
2	2693.101		⋯	5–6	2693.103	1 0 0
3	2991.70		⋯	7–8	2991.76	0 1 0
	⋯	2	3188.35	9–10	3188.26	1 0 1
4	3287.85		⋯	11–12	3287.99	0 0 2
	⋯	3	3445.97	13–14	3443.89	0 1 1
5	3633.01		⋯	15–16	3633.70	1 0 2
6	3648.35		⋯	17–18	3659.65	1 1 0
	⋯	4	3675.99	19–20	3673.67	⋯
7	3862.37		⋯	21–22	3835.63	⋯
8	3882.82		⋯	23–24	3869.5	⋯
	⋯	5	3907.66	25–26	3944.0	⋯
	⋯	6	3965.22	27–28	3961.2	⋯
9	4005.42		⋯	29–30	4042	⋯
10	4043.06		⋯	31–32	4054	⋯
11	4084		⋯	33–34	4094	⋯

ferent symmetry operators on the hyperspherical coordinates is shown,[20–23] as well as on the electronic coordinates, x_i, y_i, z_i, referred to the same body-fixed frame.

For the electronic coordinates the effect of the symmetry operations of the Complete Nuclear Permutation and Inversion Group behaves either as the identity, E, or as the reflection through the $x-y$ body-fixed frame, $\hat{\sigma}_{xy}^{\rm bf}$, or as the rotation around the y body-fixed axis, $\hat{C}_2^{\rm bf}(y)$. Therefore, the electronic wave functions should be classified according to these two latter symmetry operations as Φ_{σ,C_2}^{2S+1} (where S is the total electronic spin) such that $\hat{\sigma}_{xy}^{\rm bf}\,\Phi_{\sigma,C_2}^{2S+1}=\sigma\,\Phi_{\sigma,C_2}^{2S+1}$ and $\hat{C}_2^{\rm bf}(y)\,\Phi_{\sigma,C_2}^{2S+1}=C_2\,\Phi_{\sigma,C_2}^{2S+1}$. Doing the electronic calculations in the C_s group, the A' (A'') states correspond to $\sigma=+1(-1)$. To analyze the effect of the $\hat{C}_2^{\rm bf}(y)$ operation we examine the properties of the state at the collinear configuration as $C_2=\sigma\cdot i$. In the case under study, the $^3A'$ state corresponds to a $^3\Sigma_u^+$ (with $\sigma=+1, i=-1$), i.e., $\sigma=+1$ and $C_2=-1$. In addition, at equilateral triangular configurations this state appears to be degenerated, belonging to an E' representation of the D_{3h} symmetry point group due to the equivalent positions of the identical nuclei within the $x-y$ body-fixed plane.

Following paper I, the generalized symmetry adapted wave functions are of the form

$$\mathcal{W}_{\Omega n}^{JM\Gamma S\sigma C_2}=A_{\Omega n}^{J\Gamma S\sigma C_2}W_{\Omega n}^{JM\Gamma S\sigma C_2}+B_{\Omega n}^{J\Gamma S\sigma C_2}W_{-\Omega -n}^{JM\Gamma S\sigma C_2}, \quad (2)$$

where

$$W_{\Omega n}^{JM\Gamma S\sigma C_2}=\sqrt{\frac{2J+1}{8\pi^2}}D_{M\Omega}^{J*}(\alpha,\beta,\gamma)\frac{e^{in\phi_\tau}}{\sqrt{2\pi}}\Phi_{\sigma,C_2}^{2S+1}, \quad (3)$$

the $D_{M\Omega}^{J*}$ being Wigner rotation matrices. In Eq. (2) the $A_{\Omega n}^{J\Gamma S\sigma C_2}$ and $B_{\Omega n}^{J\Gamma S\sigma C_2}$ coefficients are given by

$$\begin{aligned}A_{\Omega n}^{J\Gamma S\sigma C_2}\propto{}&\chi^\Gamma(E)+2\cos(4n\pi/3)\chi^\Gamma(C_3)\\&+\sigma(-1)^\Omega\chi^\Gamma(E^*)\\&+\sigma(-1)^\Omega 2\cos(4n\pi/3)\chi^\Gamma(S_3),\end{aligned} \quad (4)$$

$$\begin{aligned}B_{\Omega n}^{J\Gamma S\sigma C_2}\propto{}&C_2(-1)^J[1+2\cos(2n\pi/3)]\\&\times\{(-1)^\Omega\chi^\Gamma(C_2)+\sigma\chi^\Gamma(\sigma_v)\}\end{aligned}$$

for $\Omega\neq 0$ and/or $n\neq 0$, while for $\Omega=n=0$,

$$\begin{aligned}A_{\Omega n}^{J\Gamma S\sigma C_2}\propto{}&\chi^\Gamma(E)+3C_2(-1)^J\chi^\Gamma(C_2)+2\chi^\Gamma(C_3)\\&+\sigma\chi^\Gamma(E^*)+3\sigma C_2(-1)^J\chi^\Gamma(\sigma_v)\\&+2\sigma\chi^\Gamma(S_3),\\B_{\Omega n}^{J\Gamma S\sigma C_2}={}&0,\end{aligned} \quad (5)$$

where $\chi^\Gamma(\mathcal{C})$ is the character of the symmetry operator class $\mathcal{C}$ for the Γ representation of the D_{3h} group, isomorphic with the $S_3\otimes C_i$ group. Also, $n+\Omega$ must be even because the angle γ and ϕ_γ are considered to be defined in the $[0,2\pi]$ interval instead of $[0,\pi]$ for convenience, so that the configuration space is scanned twice.

The remainder of the method is essentially the same as described in paper I. For θ, instead of exact hyperspherical harmonics, we use functions which fulfill the proper regular behavior near $\theta=0$ and $\theta=\pi/2$ for the Hamiltonian terms diagonal in Ω, thus avoiding the Eckart singularities. Also $V_{\rm ref}$, defined in Eq. (15) of paper I to evaluate the numerical basis set function in the hyperradius, is $V_{\rm ref}\equiv V(\rho,\theta=\pi/2,\phi_\tau=\pi/2)$ in this case. In Table V we present the vibronic states obtained for $J=0$. Even when the only good quantum numbers associated with each eigenstate are the total angular momentum, J, and the symmetry, characterized by the Γ irreducible representation of the $S_3\otimes C_i$ group (isomorphic with the D_{3h} group), in Table V the (v_1,v_2,v_3) quantum numbers are also assigned. Using these coordinates makes the assignment particularly simple since the asymmet-

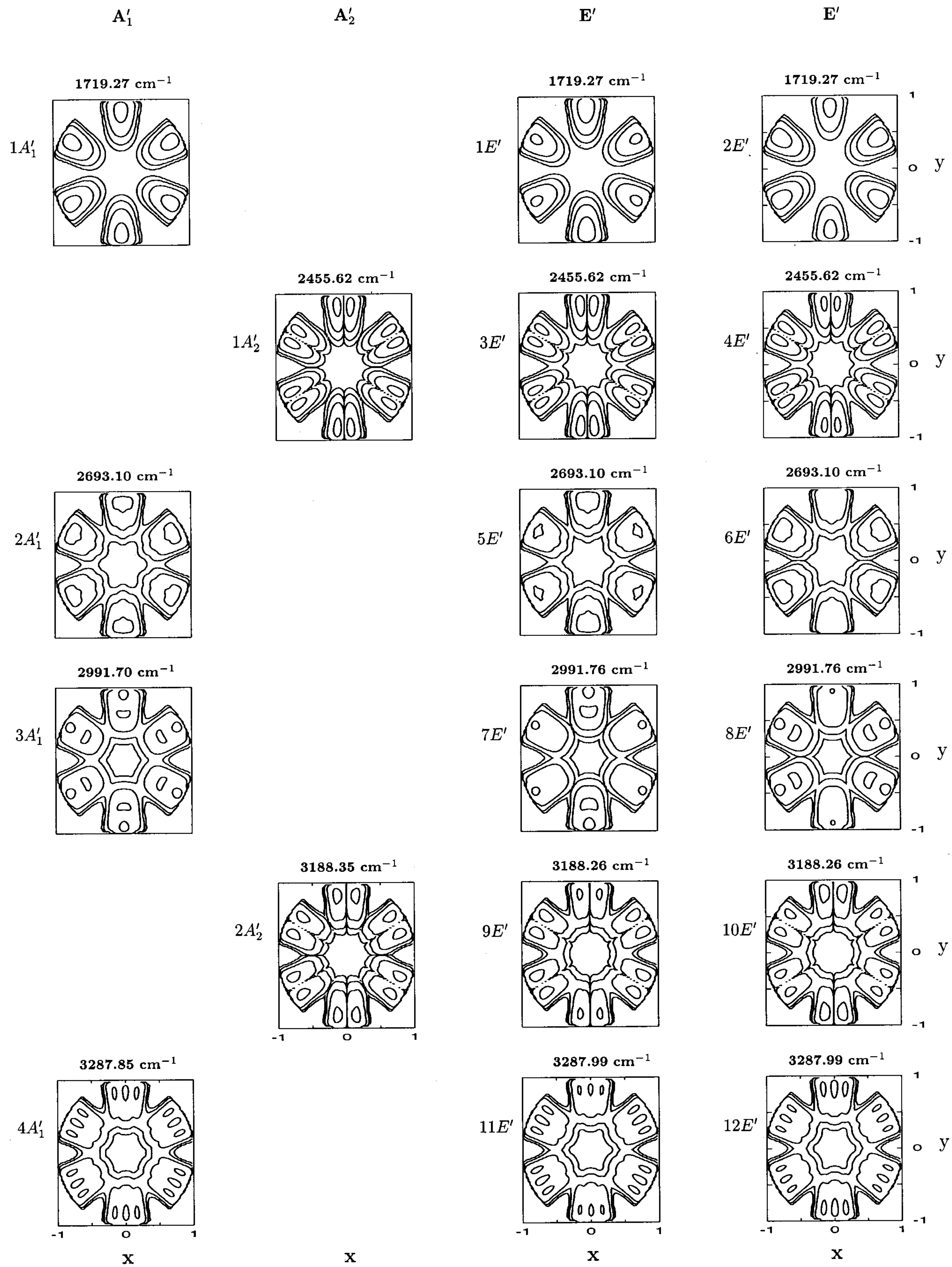

FIG. 4. Probability density contour plots in hyperspherical coordinates (ρ distance fixed at 4.57 bohr, see Fig. 2, intermediate panel, for the potential) corresponding to the six lower energy rovibrational levels that are close to triple degenerate. From top to bottom each row of panels corresponds to each rovibrational level from lower to higher energy and the three states considered. The solid curves are contours of the probability density corresponding to 0.9, 10^{-2}, 10^{-4}, and 10^{-6}. x and y have been defined as in Fig. 2.

TABLE VI. Harmonic frequencies ω_e (in cm^{-1}) for H_3^+ $(^3\Sigma_u^+)$.

Mode	Reference 4	Reference 5	Reference 6	This work
σ_g^+	1191	1233	1234.7	1235.46
σ_u^+	683	826	823.1	822.75
π_u	775	715	719.8	719.15

ric stretch, v_1, corresponds to the motion along the ρ coordinate, the symmetric stretch v_2 corresponds to the θ coordinate, while the degenerate stretch v_3 typical of a linear molecule is associated with ϕ_τ, and all of the excitation is rather well separated, at least for low excitations, as can be seen in Fig. 4. Note that the assignment for $J=0$ is particularly simplified by the fact that the excitation of each of these modes should belong to a particular irreducible representation. Also, the electronic part behaves as if it belongs to A_2', which explains why the excitation on ρ has A_2' character, while for the ground singlet state $^1A'$ of H_3^+, studied in paper I, it corresponds to the totally symmetric A_1' representation. (Similar arguments hold for the other modes.) The irreducible representation assigned to each vibronic state in Table V corresponds to the vibrational and electronic part and in order to obtain the pure vibrational character it should be multiplied by the A_2' character.

The nuclear spin of the H_3^+ nuclei is 1/2 and the total wave functions, including nuclear spin, must be antisymmetric under exchange of any pair of nuclei, according to the Fermi–Dirac statistic.[24] This implies that the rovibronic wave function (without the nuclear spin part) must be A_2' or A_2'' for total nuclear spin $I=3/2$ (*ortho* H_3^+) and E' or E'' for $I=1/2$ (*para* H_3^+). Therefore, the only existing levels in Table V are A_2' and E', while those of A_1' character do not exist. However, for total angular momentum different from zero, the vibrational states assigned for $J=0$ split into several states belonging to different representations. Hence, the interest of showing the $A_1', J=0$ eigenvalues is that they provide an idea of the frequency of the band associated to transitions with such states participate.

If we take into account that the maximum difference between the rovibrational levels obtained with our ground-state GPES and the ''experimental'' ones was of the order of 1–2 cm^{-1} (see paper I), for the present first triplet excited-state GPES we assume a similar error. From this table we can see that for the lower vibrational levels there is a near degeneracy of three, where one state is A_1' or A_2' and the other two are always E'. When we go through higher vibrational levels, in particular those corresponding to energies above the interconversion barrier [but below the asymptotic energy: $H_2^+(X\,^2\Sigma_g^+,\ v=0)+H(^2S)$, i.e., 4101 cm^{-1}], the splitting between the E' energies and the energy of the remaining irreducible representation (A_1' or A_2') is larger. We must stress that, in spite of the assumed error in the energy levels, the analytical treatment of the symmetry throughout the calculations makes feasible a very high splitting accuracy. Therefore, as we can see from the first row in Table V, corresponding to the first vibronic level, the splitting between the A_2' and E' energies is practically negligible (lower than 10^{-4} cm^{-1}).

Moreover, the energy corresponding to this first vibrational level (about 1719 cm^{-1}) may be compared with previous calculations using the harmonic approximation (about 1749 cm^{-1}, using the harmonic frequencies given by Preiskorn *et al.*[6]) giving a difference of about 30 cm^{-1}. This difference is due to the anharmonicity of the surface that makes the harmonic approximation unreliable. In Table VI we give a comparison of the harmonic frequencies obtained previously[4–6] with those obtained using the GPES reported here using the harmonic approximation. As we can see from Table VI our results are fairly good when compared with the best results previously reported.[6]

In the second vibronic level (see the second row in Table V) the splitting between the A_1' and E' energies is about 2×10^{-3} cm^{-1}. These two energy levels are the only ones sustained by the interconversion barrier (2640 cm^{-1}). However, the third vibronic level at about 2693 cm^{-1} (i.e., over the interconversion barrier between the three minima) also has a splitting between the A_2' and E' energies of about 2×10^{-3} cm^{-1}. However, when we go through higher rovibrational levels the splitting becomes larger with a clear breakage of degeneracy for the latest ones.

Finally, in Fig. 4 we have plotted the probability densities corresponding to the six lower energy vibrational levels grouped by irreducible representations for a fixed ρ value (4.57 bohr) corresponding to the three minima. In each panel of Fig. 4 we have only four contourplots of probability densities: 0.9, 10^{-2}, 10^{-4}, and 10^{-6}. If we pay our attention to the first row of panels in Fig. 4, corresponding to the probability densities of the first vibrational level, we can see no contourplots joining the different minima, indicating a very low likelihood of tunneling between the three symmetry-related minima. A similar result is obtained for the second vibrational level (the second row in Fig. 4). This result is in disagreement with previous predictions (not based on vibrational calculations) of Wormer and de Groot.[7] However, for higher vibrational levels, above the interconversion barrier (see the third to the sixth rows in Fig. 4), there are one or more contourplots joining the three minima.

V. CONCLUSIONS

In this paper we have reported a new global potential energy surface for the first triplet excited state of the H_3^+ system, based on a huge number of full configuration interaction energies, covering all the regions of the potential surface. The rms error of this GPES has been estimated to be about 27 cm^{-1} for energies below dissociation into the three separated atoms (25469 cm^{-1}) or only about 5 cm^{-1} for energies below the dissociation channel $H_2^+(X\,^2\Sigma_g^+)+H$ (^2S). The global fit is totally symmetric with respect to permutations of the hydrogen atoms. We have also reported a total of 45 bound vibrational levels (and 6 A_1' eigenvalues that do not exist) with an error estimation of about 2 cm^{-1} based on previous calculations on the ground state. We therefore conclude that the accuracy of the present GPES is very high, especially taking into account its ''global character.''

We have also found that the energy required to cross the barrier between linear structures with the atom ordering permuted (the interconversion barrier) is greater than the zero-point energy. Moreover, we have compared our zero-point energy with that obtained using the harmonic approximation[6] with a difference of only 30 cm^{-1} (both of them being lower than the interconversion barrier). This result is in disagreement with previous predictions,[1] (based on that the surface was too flat) that have considered that ''the energy required to cross the barrier between linear structures with the atom ordering permuted is less than the zero-point energy predicted by the harmonic approximation.'' Moreover, we have found two degenerate energy levels (at about 1719 and 2455 cm^{-1}), sustained by the interconversion barrier and with a very low likelihood of tunneling between the three symmetry-related minima. This result is also in disagreement with that expected by Wormer and de Groot.[7]

An important result reported in this paper is the energy splitting between the vibrational levels that are close to triple degenerate. This splitting is larger for the upper excited vibrational levels. Such splitting can provide a key feature to identify the unassigned transitions amongst the many H_3^+ lines that have been observed in hydrogen plasmas. In a forthcoming paper we plan to report rovibrational calculations for $J \neq 0$ and to obtain an analytical fit to the dipole moment corresponding to the first triplet excited state. Our aim is to compute the theoretical infrared spectrum corresponding to this state to facilitate the assignment.

ACKNOWLEDGMENTS

This work has been supported by DGICYT (Ministerio de Educación y Ciencia, Spain) under Grant Nos. PB97-0027 and PB95-0071. We want to acknowledge to CCCFC (Universidad Autónoma de Madrid) for the use of a DIGITAL parallel computer.

[1] J. Tennyson, Rep. Prog. Phys. **57**, 421 (1995).
[2] I. R. McNab, Adv. Chem. Phys. **LXXXIX**, 1 (1995).
[3] A. Carrington and R. Kennedy, J. Chem. Phys. **81**, 91 (1984).
[4] L. J. Schaad and W. V. Hicks, J. Chem. Phys. **61**, 1934 (1974).
[5] R. Ahlrichs, C. Votava, and C. Zirz, J. Chem. Phys. **66**, 2771 (1977).
[6] A. Preiskorn, D. Frye, and E. Clementi, J. Chem. Phys. **94**, 7204 (1991).
[7] P. E. S. Wormer and F. de Groot, J. Chem. Phys. **90**, 2344 (1989).
[8] A. Aguado, O. Roncero, C. Tablero, C. Sanz, and M. Paniagua, J. Chem. Phys. **112**, 1240 (2000).
[9] D. Frye, G. C. Lie, and E. Clementi, J. Chem. Phys. **91**, 2366 (1989); A. Preiskorn, *ibid.* **92**, 4941 (1990).
[10] K. A. Peterson, D. E. Woon, and T. H. Dunning, Jr. (unpublished); K. A. Peterson and D. E. Woon (unpublished); D. E. Woon and T. H. Dunning, Jr., J. Chem. Phys. **100**, 2975 (1994). Basis sets were obtained from the Extensible Computational Chemistry Environment Basis Set Database, as developed and distributed by the Molecular Science Computing Facility, Environmental and Molecular Sciences Laboratory which is part of the Pacific Northwest Laboratory, P.O. Box 999, Richland, WA 99352, and funded by the U.S. Department of Energy. The Pacific Northwest Laboratory is a multiprogram laboratory operated by Battelle Memorial Institue for the U.S. Department of Energy under Contract No. DE-AC06-76RLO 1830.
[11] See AIP document No. EPAPS: E-JCPSA6-114-308105 for *ab initio* full configuration interaction calculations for 7689 lowest triplet excited-state H_3^+ energy values and for 405 very accurate cc-pV6Z energy values. This document may be retrieved via the EPAPS homepage (http://www.aip.org/pubservs/epaps.html) or from ftp.aip.org in the directory /epaps/. See the EPAPS homepage for more information.
[12] A. Aguado and M. Paniagua, J. Chem. Phys. **96**, 1265 (1992).
[13] R. T Pack and G. A. Parker, J. Chem. Phys. **87**, 3888 (1987).
[14] R. T Pack and G. A. Parker, J. Chem. Phys. **90**, 3511 (1989).
[15] F. T. Smith, J. Math. Phys. **3**, 735 (1962).
[16] R. C. Whitten and F. T. Smith, J. Math. Phys. **9**, 1103 (1968).
[17] B. R. Johnson, J. Chem. Phys. **73**, 5051 (1980).
[18] B. R. Johnson, J. Chem. Phys. **79**, 1916 (1983).
[19] M. Lara, A. Aguado, M. Paniagua, and O. Roncero, J. Chem. Phys. **113**, 1781 (2000).
[20] P. Bartlett and B. J. Howard, Mol. Phys. **70**, 1001 (1990).
[21] W. Zickendraht, Ann. Phys. (N.Y.) **35**, 18 (1965).
[22] H. Mayer, J. Phys. A **8**, 1562 (1975).
[23] R. M. Whitnell and J. C. Light, J. Chem. Phys. **89**, 3674 (1988).
[24] P. R. Bunker and P. Jensen, in *Molecular Symmetry and Spectroscopy*, edited by R. H. Haynes (N.R.C., Ottawa, 1998).